



## Intramolecular exchange of coordinated and dangling phosphines in pentacarbonyl group 6 complexes of 1,1,2-tris(diphenylphosphino)ethane

Richard L. Keiter<sup>a,\*</sup>, Ping Ye<sup>a</sup>, Ellen A. Keiter<sup>a</sup>, John William Benson<sup>a</sup>, Weiyang Lin<sup>a</sup>, Douglas E. Brandt<sup>b</sup>, Joel S. Southern<sup>a</sup>, Arnold L. Rheingold<sup>c</sup>, Ilia Guzei<sup>c</sup>, Kraig A. Wheeler<sup>a</sup>, Lew W. Cary<sup>d</sup>

<sup>a</sup> Department of Chemistry, Eastern Illinois University, Charleston, IL 61920, United States

<sup>b</sup> Department of Physics, Eastern Illinois University, Charleston, IL 61920, United States

<sup>c</sup> Department of Chemistry and Biochemistry, University of California, San Diego, La Jolla, CA 92093, United States

<sup>d</sup> Department of Chemistry, University of Nevada, Reno, Reno, NV 89557, United States

### ARTICLE INFO

Dedicated with admiration and affection to Professor Arnold Rheingold for his many contributions to chemistry, his support of the undergraduate research community and on the occasion of his 70th birthday.

#### Keywords:

Group 6 pentacarbonyls  
Linkage isomerization  
Phosphine exchange  
Through-space coupling

### ABSTRACT

The linkage isomers,  $(OC)_5M[\kappa^1\text{-PPh}_2\text{CH}_2\text{CH}(\text{PPh}_2)_2]$  **1** and  $(OC)_5M[\kappa^1\text{-PPh}_2\text{CH}(\text{PPh}_2)\text{CH}_2\text{PPh}_2]$  **2** ( $M = \text{Cr}$ ,  $\text{Mo}$  and  $\text{W}$ ) exist in equilibrium at room temperature. Equilibrium constants for **1Cr**  $\rightleftharpoons$  **2Cr**, **1Mo**  $\rightleftharpoons$  **2Mo** and **1W**  $\rightleftharpoons$  **2W** at 25 °C in  $\text{CDCl}_3$  are 2.61, 5.0 and 4.74, respectively. Enthalpy favors the forward reaction ( $\Delta H = -13.5$ ,  $-12$  and  $-12.2 \text{ kJ mol}^{-1}$ , respectively) while entropy favors the reverse reaction ( $\Delta S = -37.6$ ,  $-28$  and  $-28.2 \text{ J K}^{-1} \text{ mol}^{-1}$ , respectively). Isomerization is much faster than chelation with **1Mo**  $\rightleftharpoons$  **2Mo**  $\gg$  **1W**  $\rightleftharpoons$  **2W**  $>$  **1Cr**  $\rightleftharpoons$  **2Cr**. Enthalpies of activation for **1Cr**  $\rightleftharpoons$  **2Cr** and **1W**  $\rightleftharpoons$  **2W** are 119.0 and 92.6  $\text{kJ mol}^{-1}$ , respectively, and entropies of activation are 1.4 and  $-28.2 \text{ J K}^{-1} \text{ mol}^{-1}$ , respectively. Isomerization is  $10^4$  times faster for these complexes than for  $(OC)_5M[\kappa^1\text{-PPh}_2\text{CH}_2\text{CH}_2\text{P}(\text{p-tolyl})_2]$ . A novel mechanism is proposed to account for the rate differences. The X-ray crystal structure of **2W** shows that the phosphorus atom of the short phosphine arm lies very close to a carbon atom of the  $\text{W}(\text{CO})_4$  equatorial plane (3.40 Å) which could allow “through-space” coupling, accounting in part for the observation of long-range  $J_{\text{PC}}$  and  $J_{\text{PW}}$  coupling. The X-ray structure of  $(OC)_5W[\kappa^1\text{-PPh}_2\text{C}(\text{=CH}_2)\text{PPh}_2]$  **5W** has been determined for comparison to **2W**.

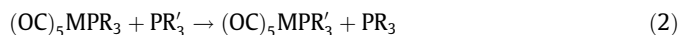
© 2010 Elsevier B.V. All rights reserved.

### 1. Introduction

Many kinetic studies have been carried out in which carbonyl groups of an organometallic complex are replaced by phosphine ligands. However, few studies involving replacement of phosphines in metal carbonyl complexes with other ligands have been reported [1]. Substitution of  $\text{Ph}_3\text{P}$  with CO is one such example.



Rate data for this slow reaction, obtained at high temperatures, allow calculation of a first-order rate constant of  $2.9 \times 10^{-9} \text{ s}^{-1}$  at 55 °C [2]. Even rarer are studies in which one phosphine is replaced by another.



At elevated temperatures such reactions are complicated by serious competition with CO loss and formation of disubstituted cis and trans products. Reaction rates at lower temperatures are too slow to be conveniently measured.

Monodentate (“dangling”) ditertiary phosphine complexes,  $(OC)_5M[\kappa^1\text{-PR}_2(\text{CH}_2)_n\text{PR}_2]$  ( $M = \text{Cr}$ ,  $\text{Mo}$  and  $\text{W}$ ), have the potential for exchange of the coordinated and uncoordinated phosphine groups, but early  $^{31}\text{P}$  NMR studies provided no evidence for this process [3]. However, their rates of chelation have been determined. The calculated  $k$  for the formation of  $(OC)_4W[\kappa^2\text{-PPh}_2\text{-}(\text{CH}_2)_2\text{PPh}_2]$  from  $(OC)_5W[\kappa^1\text{-PPh}_2(\text{CH}_2)_2\text{PPh}_2]$  is  $3 \times 10^{-10} \text{ s}^{-1}$  at 55 °C [3b]. This and similar slow reactions led to the view that an uncoordinated phosphine is inactive unless subjected to thermal or photolytic conditions that induce chelation by first severing the M–CO bond.

At first glance the polydentate ligand,  $\text{Ph}_2\text{PCH}_2\text{CH}(\text{PPh}_2)_2$  (tpe), would not be expected to exhibit unusual chemistry. It forms chelated carbonyl complexes with both four- and five-membered rings, as anticipated, and under mild conditions can function as a unidentate ligand. Reaction of tpe with  $(OC)_5W(\text{THF})$  leads to linkage isomers,  $(OC)_5W[\kappa^1\text{-PPh}_2\text{CH}_2\text{CH}(\text{PPh}_2)_2]$  **1W** and  $(OC)_5W[\kappa^1\text{-PPh}_2\text{CH}(\text{PPh}_2)\text{CH}_2\text{PPh}_2]$  **2W**, that can be obtained free of chelated and bridged products [4].

The discovery that **1W** exists in equilibrium with **2W** at room temperature and undergoes phosphine exchange much faster than expected ( $k = 3.7 \times 10^{-4} \text{ s}^{-1}$  at 55 °C), and two orders of magnitude faster than chelation, has led to a reconsideration of

\* Corresponding author. Tel.: +1 217 345 3462.

E-mail address: rlkeiter@eiu.edu (R.L. Keiter).

the substitution inertness of dangling phosphine carbonyl complexes of tungsten (Scheme 1) [5]. The uncoordinated phosphine is more than a spectator; it takes its turn at coordination.

Not all dangling phosphine complexes isomerize at unusually fast rates. The isomerization of **3W** ( $k = 2 \times 10^{-8} \text{ s}^{-1}$  at 55 °C) (Scheme 2) is four orders of magnitude slower than that of **1W** and more in line with expectation [6].

Isomerization of both **1W** and **3W** proceed by mechanisms involving transition states in which bond-making is more important than bond-breaking as shown by activation parameters, but significant mechanistic differences must exist between the two reactions [5]. We have previously suggested that phosphine exchange is accelerated in **1W** because of the presence of two dangling arms, one to weaken the W–P bond and the second to replace the coordinated phosphine. In the present work our earlier mechanism has been modified and more fully developed to give a consistent model for phosphine exchange.

We also previously noted that the phosphorus of the shorter dangling phosphine in **2W** is coupled to carbon of the *cis* carbonyl groups. Long-range coupling ( $^4J_{PC}$ ) to the *trans* carbonyl is not observed nor is any long-range P–C coupling observed for **1W**, **3W** or **4W**. The observed coupling in **2W** was postulated to have a significant “through-space” component [5].

We now report a kinetic and thermodynamic study of phosphorus exchange in two sets of linkage isomers:  $(\text{OC})_5\text{M}[\kappa^1\text{-PPh}_2\text{CH}_2\text{CH}(\text{PPh}_2)_2]$  **1M** and  $(\text{OC})_5\text{Cr}[\kappa^1\text{-PPh}_2\text{CH}(\text{PPh}_2)\text{CH}_2\text{PPh}_2]$  **2M** (M = Cr, Mo) (Scheme 3).

In addition, we have obtained the X-ray crystal structures of **2W** and  $(\text{OC})_5\text{W}(\kappa^1\text{-PPh}_2(\text{=CH}_2)\text{PPh}_2)$  **5W** and provide evidence that conformations in solution and solid state are similar.

## 2. Experimental

### 2.1. Materials and instrumentation

All reactions were carried out under a dry nitrogen atmosphere using standard Schlenk techniques. The compounds,  $(\text{Ph}_2\text{P})_2\text{C}=\text{CH}_2$  [7],  $\text{Cl}_2\text{Pt}(\text{PPh}_2)_2\text{C}=\text{CH}_2$  [8a],  $(\text{OC})_5\text{CrPPh}_2\text{H}$  [9],  $(\text{OC})_5\text{Mo}(\text{C}_5\text{H}_9\text{NH})$  [10],  $(\text{OC})_5\text{WNH}_2\text{Ph}$  [11] and  $\text{Ph}_2\text{PCH}_2\text{CH}(\text{PPh}_2)_2$  [4,12] were prepared according to literature procedures. Phosphorus-31 NMR spectra (referenced to 85% phosphoric acid) and carbon-13 NMR spectra (referenced to TMS) of  $\text{CDCl}_3$  solutions were recorded with

a GE QE-300 NMR spectrometer. Infrared spectra of  $\text{CHCl}_3$  solutions were recorded with a Nicolet 20 DXB FT-IR spectrometer. Elemental analyses were performed at the University of Illinois Microanalytical Laboratory in Urbana, Illinois.

### 2.2. Syntheses

Linkage isomers **1Cr** and **2Cr** were prepared by utilizing  $\text{PtCl}_2$  as a protecting group (Scheme 4).

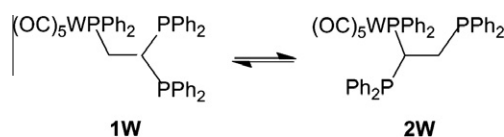
#### 2.2.1. $\text{Cl}_2\text{Pt}[\mu\text{-}(\text{PPh}_2)_2\text{CHCH}_2\text{PPh}_2]\text{Cr}(\text{CO})_5$ **6Cr**

A mixture  $\text{Cl}_2\text{Pt}(\text{PPh}_2)_2\text{C}=\text{CH}_2$  (1.15 g, 1.74 mmol),  $(\text{OC})_5\text{CrPPh}_2\text{H}$  (0.656 g, 1.74 mmol) and  $\text{KO}^t\text{Bu}$  (0.10 g, 0.89 mmol) was dissolved in 40 mL of dry THF and refluxed for 2 h. The residue remaining after solvent removal was crystallized from a 1:1 solution of  $\text{CH}_2\text{Cl}_2/\text{CH}_3\text{OH}$  to give 0.930 g (51.5%) of light yellow crystals (dec 180–182 °C). IR:  $\nu_{\text{CO}}$  1940(s)  $\text{cm}^{-1}$ , 2065(m)  $\text{cm}^{-1}$ .  $^{31}\text{P}\{^1\text{H}\}$  NMR:  $\delta$  57.4 ppm (t,  $^3J_{\text{PP}} = 4.50$  Hz),  $\delta$  –36.9 ppm (d,  $J_{\text{PtP}} = 3077$  Hz,  $^3J_{\text{PP}} = 4.50$  Hz). Anal. Calc. for  $\text{C}_{43}\text{H}_{33}\text{Cl}_2\text{O}_5\text{P}_3\text{PtW}$ : C, 49.63; H, 3.20. Found: C, 49.60; H, 3.30%.

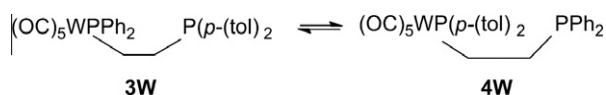
#### 2.2.2. $(\text{OC})_5\text{Cr}[\kappa^1\text{-PPh}_2\text{CH}_2\text{CH}(\text{PPh}_2)_2]$ **1Cr** and $(\text{OC})_5\text{Cr}[\kappa^1\text{-PPh}_2\text{CH}(\text{PPh}_2)\text{CH}_2\text{PPh}_2]$ **2Cr** [4]

A mixture of **6Cr** (0.705 g, 0.677 mmol) and KCN (0.176 g, 2.71 mmol) in ethanol (50 mL) was stirred for 54 h at room temperature. The yellow cloudy mixture was taken to dryness and the resulting residue was extracted with  $\text{CH}_2\text{Cl}_2$  (30 mL, two aliquots). The volume of the solution was reduced by half and an equal volume of  $\text{CH}_3\text{OH}$  was added. After 2 h at –5 °C, the solution was filtered and the filtrate was taken to dryness and chromatographed on alumina (80–200 mesh, neutral deactivated) with a 2:3 dichloromethane/hexane solution. The first yellow band was collected and, after solvent removal, the resulting solid was crystallized from  $\text{CH}_2\text{Cl}_2/\text{CH}_3\text{OH}$  to give a yellow solid consisting of a 1:2 mixture of **1Cr** and **2Cr** (0.210 g, 40.1%). **1Cr**:  $^{31}\text{P}\{^1\text{H}\}$  NMR:  $\delta$  51.5 ppm (t,  $^3J_{\text{PP}} = 2.8$  Hz),  $\delta$  –3.0 ppm (d,  $^3J_{\text{PP}} = 2.8$  Hz);  $^{13}\text{C}\{^1\text{H}\}$  NMR  $\delta$  216.4 ppm (d,  $^2J_{\text{PC}(\text{cis})} = 12.9$  Hz),  $\delta$  221.8 ppm (d,  $^2J_{\text{PC}(\text{trans})} = 6.9$  Hz). **2Cr**:  $^{31}\text{P}\{^1\text{H}\}$  NMR:  $\delta$  68.5 (dd,  $^2J_{\text{PP}} = 194.2$  Hz,  $^3J_{\text{PP}} = 20.1$  Hz),  $\delta$  –11.2 ppm (d,  $^2J_{\text{PP}} = 194.2$  Hz),  $\delta$  –15.8 ppm (d,  $^3J_{\text{PP}} = 20.1$  Hz)  $^{13}\text{C}\{^1\text{H}\}$  NMR  $\delta$  216.3 ppm (dd,  $^2J_{\text{PC}(\text{cis})} = 12.5$  Hz,  $^4J_{\text{PC}(\text{cis})} = 3.4$  Hz),  $\delta$  221.7 ppm (d,  $^2J_{\text{PC}(\text{trans})} = 5.1$  Hz).

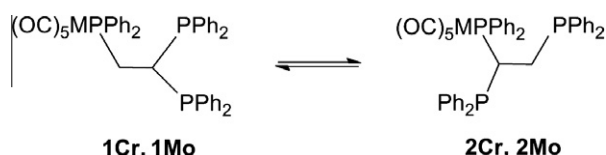
The isomeric mixture of **1Cr** and **2Cr** in a 1:2 ratio was also generated with a palladium dichloride protecting group by procedures identical to those described for the platinum analogues (29.9%) (Scheme 4).  $\text{Cl}_2\text{Pd}(\text{PPh}_2)_2\text{C}=\text{CH}_2$  (85%):  $^{31}\text{P}\{^1\text{H}\}$  NMR  $\delta$



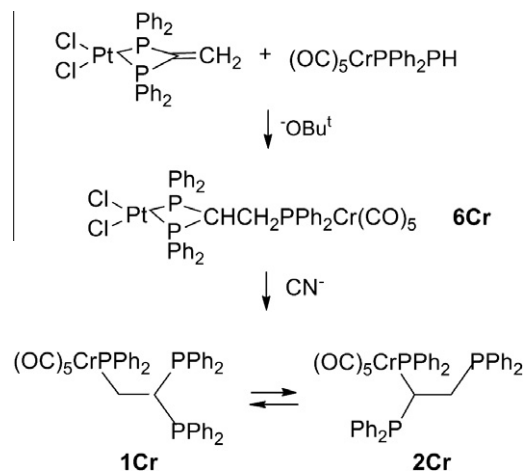
Scheme 1.



Scheme 2.



Scheme 3.



Scheme 4.

–20.6 ppm.  $\text{Cl}_2\text{Pd}[\mu\text{-}(\text{PPh}_2)_2\text{CHCH}_2\text{PPh}_2]\text{Cr}(\text{CO})_5$  (61%): IR  $\nu_{\text{CO}}$  1939(s)  $\text{cm}^{-1}$ , 2065(m)  $\text{cm}^{-1}$ ;  $\delta$  –27.2 ppm (d,  $^3J_{\text{PP}} = 3.2$  Hz),  $\delta$  57.4 ppm (t,  $^3J_{\text{PP}} = 3.2$  Hz).

### 2.2.3. $(\text{OC})_5\text{Mo}[\kappa^1\text{-PPh}_2\text{CH}_2\text{CH}(\text{PPh}_2)_2]$ **1Mo** and $(\text{OC})_5\text{Mo}[\kappa^1\text{-PPh}_2\text{CH}(\text{PPh}_2)_2\text{CH}_2\text{PPh}_2]$ **2Mo** [4]

A mixture of  $(\text{OC})_5\text{Mo}(\text{C}_5\text{H}_{10}\text{NH})$  (0.372 g, 1.16 mmol) and  $\text{Ph}_2\text{PCH}_2\text{CH}(\text{PPh}_2)_2$  (0.674 g, 1.16 mmol) was dissolved in toluene (10 mL) and stirred at room temperature for 24 h. The solvent was removed under vacuum to give an oily residue that was dissolved in 2 mL of  $\text{CH}_2\text{Cl}_2$  and 8 mL of  $\text{CH}_3\text{OH}$  and kept at  $-5^\circ\text{C}$  for 24 h. A yellow solid was collected which was shown by  $^{31}\text{P}\{^1\text{H}\}$  NMR to be a mixture of **1Mo**, **2Mo** and chelated complexes. The mixture was chromatographed on alumina (80–200 mesh, neutral deactivated) with  $\text{CH}_2\text{Cl}_2/n$ -hexane solvent (1:2) to give in the first yellow band a mixture of **1Mo** and **2Mo** (0.63 g, 66%).  $^{31}\text{P}\{^1\text{H}\}$  NMR: **1Mo**:  $\delta$  31.5 ppm (t,  $^3J_{\text{PP}} = 8.4$  Hz),  $\delta$  –3.9 ppm (d,  $^3J_{\text{PP}} = 8.6$  Hz)  $^{31}\text{P}\{^1\text{H}\}$  NMR: **2Mo**:  $\delta$  50.5 (dd,  $^2J_{\text{PP}} = 214.2$  Hz,  $^3J_{\text{PP}} = 19.7$  Hz),  $\delta$  –10.0 ppm (d,  $^2J_{\text{PP}} = 214.2$  Hz),  $\delta$  –15.9 ppm (d,  $^3J_{\text{PP}} = 19.7$  Hz). The second band contained chelated complexes [4].  $^{31}\text{P}\{^1\text{H}\}$  NMR:  $(\text{OC})_4\text{Mo}[\kappa^2\text{-}(\text{PPh}_2)_2\text{CHCH}_2\text{PPh}_2]$ :  $\delta$  28.1 ppm (d,  $^3J_{\text{PP}} = 7.3$  Hz), –18.3 ppm (t,  $^3J_{\text{PP}} = 7.3$  Hz);  $(\text{OC})_4\text{Mo}[\kappa^2\text{-PPh}_2\text{CH}(\text{PPh}_2)\text{CH}_2\text{PPh}_2]$ :  $\delta$  65.4 ppm (dd,  $^2J_{\text{PP}} = 23.8$  Hz,  $^3J_{\text{PP}} = 10.5$  Hz),  $\delta$  48.1 (dd,  $^3J_{\text{PP}} = 10.5$  Hz,  $^3J_{\text{PP}} = 2.4$  Hz),  $\delta$  –14.3 ppm (d,  $^2J_{\text{PP}} = 23.8$  Hz,  $^3J_{\text{PP}} = 2.4$  Hz).

### 2.2.4. $(\text{OC})_5\text{W}[\kappa^1\text{-PPh}_2\text{C}(\text{=CH}_2)\text{PPh}_2]$ **5W** and $[(\text{OC})_5\text{WPPH}_2]_2\text{C}=\text{CH}_2$ **7W**

A mixture of  $(\text{Ph}_2\text{P})_2\text{C}=\text{CH}_2$  (0.95 g, 2.4 mmol) and  $\text{W}(\text{CO})_5\text{NH}_2\text{Ph}$  (1.4 g, 3.4 mmol) in toluene (30 mL) was stirred for 24 h. The solvent was removed and the resulting yellow residue was recrystallized from  $\text{CH}_2\text{Cl}_2/\text{CH}_3\text{OH}$  to give light brown crystals that were purified further with silica gel (80–200 mesh) column chromatography. The first band, eluted with ethyl acetate/petroleum ether (1:9), gave faint yellow crystals (0.71 g, 41%) of **5W**. IR:  $\nu_{\text{CO}}$  1940(s)  $\text{cm}^{-1}$ , 2071(m)  $\text{cm}^{-1}$ .  $^1\text{H}$  NMR:  $\delta$  5.9 ppm (dd,  $^3J_{\text{PH}(\text{trans})} = 44.0$  Hz,  $^3J_{\text{PH}(\text{cis})} = 6.2$  Hz;  $^2J_{\text{HH}}$  unobserved as established by a COSY spectrum). The second vinyl hydrogen resonance was hidden by that of phenyl protons.  $^{31}\text{P}\{^1\text{H}\}$  NMR:  $\delta$  –12.1 ppm (d,  $^2J_{\text{PP}} = 68.4$  Hz),  $\delta$  = 30.2 ppm (d,  $^2J_{\text{PP}} = 68.4$  Hz,  $^1J_{\text{WP}} = 245.9$  Hz).  $^{13}\text{C}\{^1\text{H}\}$  NMR:  $\delta$  199.2 ppm ( $^2J_{\text{PC}(\text{ax})} = 22.5$  Hz),  $\delta$  197.3 ppm ( $^2J_{\text{PC}(\text{eq})} = 7.0$  Hz,  $^1J_{\text{WC}} = 126.3$  Hz),  $\delta$  144.7 ppm ( $^1J_{\text{CP}(1)} = 19.5$  Hz,  $^1J_{\text{CP}(2)} = 46.5$  Hz),  $\delta$  144.5 ppm ( $^2J_{\text{CP}(1)} = 1.1$  Hz, 15.5 Hz,  $^2J_{\text{CP}(2)} = 15.5$  Hz). A HETCOR NMR spectrum and attached proton test (APT) were used to assign the vinyl carbon atoms.

The dimetallic complex **7W** was obtained by stirring a mixture of  $(\text{Ph}_2\text{P})_2\text{C}=\text{CH}_2$  (0.48 g, 1.2 mmol) with  $(\text{OC})_5\text{WNH}_2\text{Ph}$  (1.5 g, 3.6 mmol) in toluene (15 ml) for 7 days. The dark green oil that resulted upon solvent removal was crystallized from  $\text{CH}_2\text{Cl}_2/\text{CH}_3\text{OH}$  and chromatographed over silica gel (80–200 mesh). The first product, isolated from 1:9 ethyl acetate/petroleum ether, was shown to be compound **5W** while the second was identified as **7W**. Recrystallization of **7W** from  $\text{CH}_2\text{Cl}_2/\text{CH}_3\text{OH}$  gave faint yellow crystals (0.22 g, 17%). IR:  $\nu_{\text{CO}}$  1944(s)  $\text{cm}^{-1}$ , 2071(m)  $\text{cm}^{-1}$ .  $^{31}\text{P}\{^1\text{H}\}$  NMR:  $\delta$  36.2 ppm (simulation results for ABX pattern:  $^2J_{\text{PP}} = 20.2$  Hz,  $^1J_{\text{WP}} = 248.8$  Hz,  $^3J_{\text{WP}} = 1.6$  Hz). Anal. Calc. for  $\text{C}_{36}\text{H}_{22}\text{O}_{10}\text{P}_2\text{W}_2$ : C, 41.41; H, 2.12. Found: C, 41.56; H, 2.24%.

## 2.3. Equilibrium and kinetics measurements

Isomer ratios for kinetic runs and equilibrium constants were determined from integrations of  $^{31}\text{P}\{^1\text{H}\}$  NMR spectra. The spectra were first order and no signals overlapped. A mixture of **1Cr** and **2Cr** (56.0 mg, 72.3 mmol) and  $\text{CDCl}_3$  (0.50 mL) was flame sealed under vacuum at liquid nitrogen temperature in an NMR tube, thawed and thermostated in a constant temperature bath at the

appropriate temperature. In a similar fashion a mixture of **1Mo** and **2Mo** (45.0 mg, 54.9 mmol) in  $\text{CDCl}_3$  (0.50 mL) was prepared. The NMR probe was brought to the same temperature as the bath and the  $^{31}\text{P}\{^1\text{H}\}$  NMR spectrum was recorded. Integrations were performed as described previously [5]. Equilibrium was assumed to have been reached when the integral ratio of isomers remained unchanged after three consecutive runs spaced by several days. Reactions could be shifted in the forward and reverse directions by changing the temperature.

## 2.4. Crystallographic structure determinations

Crystal, data collection and refinement parameters for **2W** and **5W** are given in Table 1. Crystals of **2W** and **5W** were obtained by layering a  $\text{CH}_2\text{Cl}_2$  solution with  $\text{CH}_3\text{OH}$  in an NMR tube and allowing the layers to slowly diffuse at  $0^\circ\text{C}$ . Crystals of **5W** required no special care but those of **2W** go to powder rather rapidly on solvent loss. This problem was solved by mounting a crystal of **2W** on a fine glass fiber with mineral oil and immediately placing it in the cold stream. The asymmetric unit contains a molecule of the recrystallization solvent,  $\text{CH}_2\text{Cl}_2$ .

Systematic absences in the diffraction data uniquely identified the space groups of both **2W** and **5W**. Data for **2W** were collected on a Bruker P4 equipped with a SMART 1 K detector and were corrected for absorption by empirical methods (SADABS). Data for **5W** were collected on a Siemens P4 equipped with scintillation detector and corrected for absorption using semi-empirical procedures based on psi-scan data. Both structures were solved by direct methods, completed by successive Fourier syntheses and refined by full-matrix, least-squares methods. All non-hydrogen atoms were refined with anisotropic thermal parameters and hydrogen atoms were treated as idealized contributions. All software is contained in the SHELXTL libraries of programs (ver. 5.1, G. Sheldrick, Bruker AXS, Madison, WI).

## 3. Results and discussion

### 3.1. Thermodynamics

Equilibrium constants for isomerization of the chromium (**1Cr**  $\rightleftharpoons$  **2Cr**), molybdenum (**1M**  $\rightleftharpoons$  **2Mo**) and tungsten (**1W**  $\rightleftharpoons$  **2W**) complexes at several temperatures are presented in Table 2. Isomer ratios for the molybdenum and tungsten complexes are very nearly the same (about 5:1 at room temperature), favoring coordination of the sterically congested end of the phosphorus ligand. On a statistical basis, a ratio of 2:1 might be expected if M–P bond strengths are nearly the same. The  $[\mathbf{2Cr}]/[\mathbf{1Cr}]$  ratio is smaller than those for  $[\mathbf{2Mo}]/[\mathbf{1Mo}]$  and  $[\mathbf{2W}]/[\mathbf{1W}]$  and even drops below 2.0 at  $55^\circ\text{C}$  ( $K = 1.67$ ). It would appear that steric demands play a larger role in the complexes containing the smaller chromium atom as compared to molybdenum or tungsten atoms.

From the equilibrium constants for the isomerization reactions, values of  $\Delta H$ ,  $\Delta S$  and  $\Delta G$  were determined from van't Hoff plots ( $\ln K$  versus  $1/T$ ) (Table 3). Enthalpy favors the forward reaction while entropy favors the reverse reaction. The **1Cr**  $\rightleftharpoons$  **2Cr** reaction is slightly more exothermic than **1Mo**  $\rightleftharpoons$  **2Mo** or **1W**  $\rightleftharpoons$  **2W**, but entropy favors the reverse reaction for **1Cr**  $\rightleftharpoons$  **2Cr** more than for **1Mo**  $\rightleftharpoons$  **2Mo** or **1W**  $\rightleftharpoons$  **2W**, attributable to greater congestion in **2Cr**.

The exothermic nature of the isomerization reactions suggests that the M–P bond strength is greater in **2** than **1**. The opposite might have been predicted based on the fact that phosphines separated by two carbon atoms are more basic toward  $\text{H}^+$  than those separated by one. For example, the  $\text{p}K_{\text{a}}$ s of  $\text{Ph}_2\text{PCH}_2\text{CH}_2\text{PPh}_2$  (dppe)

**Table 1**  
Crystallographic data for **2W** and **5W**.

	<b>2W</b>	<b>5W</b>
Formula	C <sub>43</sub> H <sub>33</sub> O <sub>5</sub> P <sub>3</sub> W·CH <sub>2</sub> Cl <sub>2</sub>	C <sub>31</sub> H <sub>22</sub> O <sub>5</sub> P <sub>2</sub> W
Formula weight	991.38	720.28
T (K)	173(2)	293(2)
Crystal size (mm)	0.40 × 0.30 × 0.20	0.30 × 0.30 × 0.20
Crystal system	monoclinic	monoclinic
Space group	P2 <sub>1</sub> /c	P2 <sub>1</sub> /c
Color	colorless block	colorless block
a (Å)	14.5297(7)	13.412(5)
b (Å)	13.2818(6)	9.556(11)
c (Å)	22.3048(11)	22.435(8)
β (°)	104.5190(10)	92.77(3)
V (Å <sup>3</sup> )	4166.9(3)	2872(4)
Z	4	4
D <sub>calc</sub> (g cm <sup>-3</sup> )	1.580	1.666
μ(Mo Kα), (cm <sup>-1</sup> )	30.6	41.72
Reflections collected	18 296	4954
Independent reflections	7888	3764
Radiation	Mo Kα, λ = 0.71073 Å	Mo Kα, λ = 0.71073 Å
Goodness-of-fit (GOF) on F <sup>2</sup>	1.166	1.021
Final R indices [I > 2σ(I)]	R <sub>1</sub> = 0.0651, wR <sub>2</sub> = 0.1226	R <sub>1</sub> = 0.0306, wR <sub>2</sub> = 0.0681
R indices (all data)	R <sub>1</sub> = 0.0941, wR <sub>2</sub> = 0.1315	R <sub>1</sub> = 0.0438, wR <sub>2</sub> = 0.0736
Maximum/minimum final difference map (e Å <sup>-3</sup> )	1.129/−3.870	0.447/−1.81

**Table 2**  
Equilibrium constants for reactions **1Cr** = **2Cr**, **1Mo** = **2Mo**, **1W** = **2W** and **3Mo** = **4Mo**.

T (K)	[ <b>2Cr</b> ]/[ <b>1Cr</b> ]	[ <b>2Mo</b> ]/[ <b>1Mo</b> ]	[ <b>2W</b> ]/[ <b>1W</b> ] <sup>a</sup>	[ <b>4Mo</b> ]/[ <b>3Mo</b> ] <sup>b</sup>
283	3.60 ± 0.04	6.5 ± 1	6.14 ± 0.04	
290		5.2 ± 0.8		
298	2.61 ± 0.04	5.0 ± 0.8	4.74 ± 0.01	1.83 ± 0.04
313	2.04 ± 0.04		3.76 ± 0.05	1.86 ± 0.03
328	1.67 ± 0.02		3.01 ± 0.02	1.91 ± 0.04

<sup>a</sup> Data from [5].<sup>b</sup> Data from [6].**Table 3**  
Thermodynamic parameters, ΔH, ΔS and ΔG<sub>298K</sub>, for reactions **1Cr** = **2Cr**, **1Mo** = **2Mo**, **1W** = **2W** and **3Mo** = **4Mo**.

Reaction	ΔH (kJ mol <sup>-1</sup> )	ΔS (J K <sup>-1</sup> mol <sup>-1</sup> )	ΔG (kJ mol <sup>-1</sup> )
<b>1Cr</b> = <b>2Cr</b>	−13.6 ± 0.4	−37.6 ± 1.3	−2.4 ± 0.4
<b>1Mo</b> = <b>2Mo</b>	−12 ± 5	−28 ± 17	−4 ± 5
<b>1W</b> = <b>2W</b>	−12.2 ± 0.1	−28.2 ± 0.3	−3.9 ± 0.1
<b>3Mo</b> = <b>4Mo</b>	−1.2 ± 0.1	1.5 ± 0.4	−1.6 ± 0.4

and Ph<sub>2</sub>PCH<sub>2</sub>PPh<sub>2</sub> (dpm) are 3.86 and 3.81, respectively [13], or K for the reaction dppeH<sup>+</sup> + dpmm = dppe + dpmmH<sup>+</sup> is 0.89, i.e., unfavorable. Of course the affinity of phosphines for hydrogen ions does not account for differences in pi capacity.

It is possible that **2** is more stable than **1** because van der Waals attractions of the short dangling phosphine for the equatorial carbonyl groups of **2** provide extra stability (*vide infra*) and account to some degree for the favorable enthalpy change for these isomerizations. The enthalpy changes for isomerization are only about 12 kJ mol<sup>-1</sup>, not outside the range of van der Waals attractions.

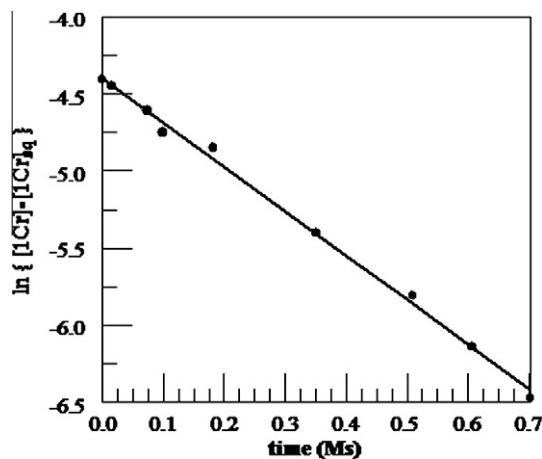
### 3.2. Kinetics

Plots such as ln{[**1Cr**]-[**1Cr**]<sub>eq</sub>} versus time (Fig. 1) allowed rate constants to be determined for the chromium, molybdenum and tungsten systems [14]. Isomerization of the molybdenum com-

plexes, even at 10 °C, was relatively fast and complicated by competing chelation reactions; as a result, their rate constants are less precisely determined than those of chromium and tungsten reactions.

Table 4 shows rate constants for forward and reverse reactions **1Cr** = **2Cr**, **1Mo** = **2Mo** and **1W** = **2W** and their half-lives to equilibrium. For comparison purposes, parallel data for **3Cr** = **4Cr**, **3Mo** = **4Mo** and **3W** = **4W** are presented. Isomerization of the molybdenum complexes is much faster than those of chromium or tungsten, fitting literature trends for substitution in group 6 carbonyl complexes [1]. For example, rate constants for the substitution of CO in M(CO)<sub>6</sub> by Ph<sub>3</sub>P at 130 °C are 1.4 × 10<sup>-4</sup>, 2.0 × 10<sup>-3</sup> and 4.0 × 10<sup>-6</sup> s<sup>-1</sup>, respectively, for Cr, Mo and W [1,15]. The order Mo > Cr > W is observed for many substitution processes [1,16]. However, the isomerization of **1W** is faster than that of **1Cr** and for **3W** it is faster than for **3Cr**.

Metal–phosphine bond strengths in group 6 carbonyl complexes have been shown to follow the order W–P > Mo–P > Cr–P [17]. The Cr–P bond energy in (CO)<sub>5</sub>CrPPh<sub>3</sub>, as determined by photoacoustic calorimetry, is 131 kJ mol<sup>-1</sup> [17a,18]. Kinetic studies yield a value of 138 kJ mol<sup>-1</sup> for Cr–P in CO<sub>5</sub>CrPPh<sub>3</sub> [2]. Thermochemical analyses lead to a bond energy of 119 kJ mol<sup>-1</sup> for Mo–P in (OC)<sub>4</sub>M(PPh<sub>2</sub>Me)<sub>2</sub> and M–P energies of 119, 153 and

Fig. 1. A plot of ln{[**1Cr**]-[**1Cr**]<sub>eq</sub>} vs. time.**Table 4**  
Rate constants for isomerization.

Reaction	T (K)	k <sub>1</sub> (s <sup>-1</sup> )	k <sub>-1</sub> (s <sup>-1</sup> )	ln2/(k <sub>1</sub> + k <sub>-1</sub> ) <sup>a</sup>
<b>1Cr</b> = <b>2Cr</b>	283	(2.04 ± 0.02) × 10 <sup>-7</sup>	(5.64 ± 0.20) × 10 <sup>-8</sup>	31 days
<b>1Cr</b> = <b>2Cr</b>	298	(2.10 ± 0.02) × 10 <sup>-6</sup>	(8.03 ± 0.29) × 10 <sup>-7</sup>	2.8 days
<b>1Cr</b> = <b>2Cr</b>	313	(1.68 ± 0.02) × 10 <sup>-5</sup>	(8.22 ± 0.17) × 10 <sup>-6</sup>	7.7 h
<b>1Cr</b> = <b>2Cr</b> <sup>b</sup>	328	(1.13 ± 0.02) × 10 <sup>-4</sup>	(7.15 ± 0.33) × 10 <sup>-5</sup>	63 min
<b>1W</b> = <b>2W</b>	283	(1.60 ± 0.04) × 10 <sup>-6</sup>	(2.61 ± 0.06) × 10 <sup>-7</sup>	4.3 days
<b>1W</b> = <b>2W</b>	298	(1.18 ± 0.01) × 10 <sup>-5</sup>	(2.50 ± 0.01) × 10 <sup>-6</sup>	13.5 h
<b>1W</b> = <b>2W</b>	313	(7.95 ± 0.30) × 10 <sup>-5</sup>	(2.11 ± 0.10) × 10 <sup>-5</sup>	2.4 h
<b>1W</b> = <b>2W</b> <sup>b</sup>	328	(4.21 ± 0.26) × 10 <sup>-4</sup>	(1.38 ± 0.08) × 10 <sup>-4</sup>	21 min
<b>1Mo</b> = <b>2Mo</b> <sup>c</sup>	283	(6 ± 3) × 10 <sup>-4</sup>	(9 ± 5) × 10 <sup>-5</sup>	17 min
<b>3Cr</b> = <b>4Cr</b> <sup>d</sup>	328	(1.23 ± 0.04) × 10 <sup>-8</sup>	(6.52 ± 0.02) × 10 <sup>-9</sup>	427 days
<b>3W</b> = <b>4W</b> <sup>d</sup>	328	(2.3 ± 0.1) × 10 <sup>-8</sup>	(9.7 ± 0.5) × 10 <sup>-9</sup>	245 days
<b>3Mo</b> = <b>4Mo</b> <sup>e</sup>	298	(1.61 ± 0.03) × 10 <sup>-7</sup>	(8.4 ± 0.3) × 10 <sup>-8</sup>	49 days
<b>3Mo</b> = <b>4Mo</b> <sup>e</sup>	313	(1.20 ± 0.03) × 10 <sup>-6</sup>	(6.48 ± 0.03) × 10 <sup>-7</sup>	6.5 days
<b>3Mo</b> = <b>4Mo</b> <sup>e</sup>	328	(7.76 ± 0.04) × 10 <sup>-6</sup>	(4.24 ± 0.04) × 10 <sup>-6</sup>	2.3 h

<sup>a</sup> Half-life to equilibrium.<sup>b</sup> Calculated from values of k at lower temperatures.<sup>c</sup> Too fast to be measured at higher temperatures.<sup>d</sup> Too slow to be measured at lower temperatures [6a].<sup>e</sup> Data from [6a].

**Table 5**

Activation parameters ( $\Delta H^\ddagger$ ,  $\Delta S^\ddagger$ ) for forward (f) and reverse (r) reactions  $1\text{Cr} = 2\text{Cr}$ ,  $1\text{W} = 2\text{W}$  and  $3\text{Mo} = 4\text{Mo}$ .

Reaction	$\Delta H^\ddagger$ (f) (kJ mol <sup>-1</sup> )	$\Delta H^\ddagger$ (r) (kJ mol <sup>-1</sup> )	$\Delta S^\ddagger$ (f) (J mol <sup>-1</sup> K <sup>-1</sup> )	$\Delta S^\ddagger$ (r) (J mol <sup>-1</sup> K <sup>-1</sup> )
$1\text{Cr} = 2\text{Cr}$	105.0 ± 0.5	119.9 ± 1.2	1.4 ± 1.6	40.4 ± 3.9
$1\text{W} = 2\text{W}$	92.6 ± 1.9	104.5 ± 1.8	-28.2 ± 6.2	-1.0 ± 6.0
$3\text{Mo} = 4\text{Mo}$	102.4 ± 0.6	103.6 ± 1.8	-32 ± 2	-33 ± 1

183 kJ mol<sup>-1</sup>, respectively, for M = Cr, Mo and W in (OC)<sub>3</sub>M (PPh<sub>2</sub>Me)<sub>3</sub>. The resulting estimated metal–phosphine bond energy ratios are 1.0:1.26:1.43 for Cr:Mo:W metal tricarbonyl phosphine complexes [17b].

If the isomerization reactions proceed by a strictly dissociative mechanism, rates would be expected to follow the order  $1\text{Cr} > 1\text{Mo} > 1\text{W}$ . The observed order,  $1\text{Mo} \gg 1\text{W} > 1\text{Cr}$ , strongly implies that the reactions have an associative component that is much more important for the complexes with the larger and similarly sized Mo and W atoms than those of Cr [16]. Activation parameters support this view (Table 5). For all three  $1\text{M}$  complexes the enthalpies of activation,  $\Delta H^\ddagger$ , are smaller than the estimated M–P bond energies (see above), suggesting a transition state in which bond-making is very important and becomes more so in descending group 6. Chromium–phosphorus bond dissociation energies are 10–15 kJ mol<sup>-1</sup> greater than the activation energy for  $1\text{Cr}$ . The difference between the W–P dissociation energy and  $\Delta H^\ddagger$  for  $1\text{W}$  is estimated to be about 80 kJ mol<sup>-1</sup>. While we were unable to determine activation energies for  $1\text{Mo}$  because of rapid decomposition rates,  $\Delta H^\ddagger$  for  $3\text{Mo}$  is also consistent with association and is about 50 kJ mol<sup>-1</sup> smaller than the estimated Mo–P dissociation energy.

The increasing importance of an associative isomerization process in going from  $1\text{Cr}$  to  $1\text{W}$  is supported by entropies of activation. For  $1\text{Cr}$ ,  $\Delta S^\ddagger$  is 1.4 J mol<sup>-1</sup> K<sup>-1</sup> while for  $1\text{W}$  it is -28.2 J mol<sup>-1</sup> K<sup>-1</sup>. The trend is in the same direction for the reverse reactions.

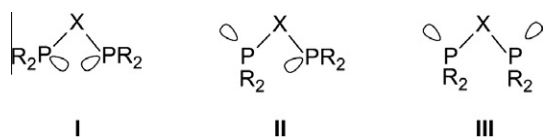
### 3.3. Solution and solid state structures; long-range P–C coupling

Geminal phosphines are found in the solid state with one of three basic conformations. The lone pairs may be pointed generally toward one another as in **I** (Scheme 5), staggered as in **II**, or pointed in opposite directions as in **III**.

The X-ray crystal structures of (Ph<sub>2</sub>P)<sub>2</sub>CHCH<sub>2</sub>PPhH (Htppe), Ph<sub>2</sub>CH<sub>2</sub>PPh<sub>2</sub> (dppm) and (Ph<sub>2</sub>P)<sub>2</sub>C=CH<sub>2</sub> (vdpp) show that Htppe and dppm adopt structure **I**, while vdpp chooses structure **II** [19–22].

The X-ray structures of **2W** and **5W** are shown in Figs. 2 and 3 and selected bond distances and bond angles are shown in Tables 6 and 7. The structure of (OC)<sub>5</sub>W[κ<sup>1</sup>-PPh<sub>2</sub>CH<sub>2</sub>PPh<sub>2</sub>] **8W** has been reported previously [22]. All three molecules have approximately C<sub>4v</sub> symmetry. The W–P distances in **2W** and **5W** are 2.5385(19) Å and 2.530(2) Å, respectively, which are statistically identical to each other and are a little longer than the W–P distance, 2.516(5) Å, in **8W**.

McFarlane's group has shown from analyses of <sup>2</sup>J<sub>PP</sub> and torsional angles that the predominant conformations of the free diphosphine



Scheme 5.

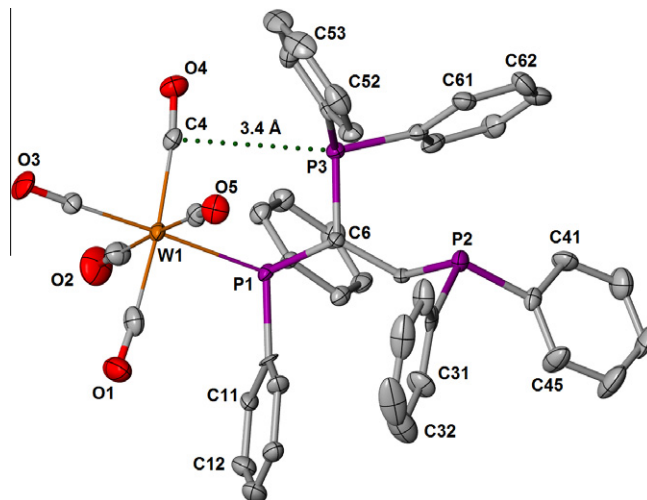


Fig. 2. Molecular structure of (OC)<sub>5</sub>W[κ<sup>1</sup>-PPh<sub>2</sub>CH(PPh<sub>2</sub>)CH<sub>2</sub>PPh<sub>2</sub>] **2W** (ORTEP, 50% thermal ellipsoid).

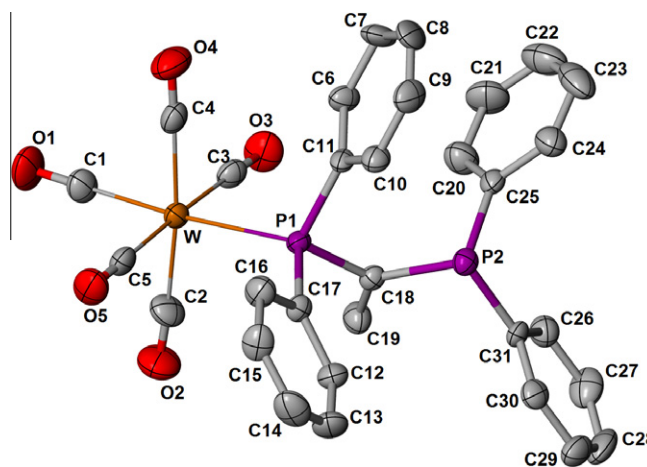


Fig. 3. Molecular structure of (OC)<sub>5</sub>W[κ<sup>1</sup>-PPh<sub>2</sub>C(=CH<sub>2</sub>)PPh<sub>2</sub>] **5W** (ORTEP, 50% thermal ellipsoid).

ligands in solution tend to be similar to those found in the solid state. Large <sup>2</sup>J<sub>PP</sub> values are associated with type **I**, intermediate values with type **II** and small values with type **III** [7,23].

The conformations exhibited by the free ligands in solid state and solution are also observed for the W(CO)<sub>5</sub> complexes, with **2W** and **8W** having conformation **I** and **5W** belonging to type **II** (Scheme 6). Thus only small changes in ligand orientation are required for coordination.

The P–C–P angle in free dppm is 106.2° and, upon formation of **8W**, it opens to 111.5°. This is the smallest angle among many that have been reported for dangling dppm complexes [22,24]. It is assumed that the P–C–P bond angle in Htppe (105.1°) is very similar to that in tppe. Surprisingly the P–C–P angle of tppe is reduced to 103.3° when coordinated in **2W**. It is noteworthy that the P–C–P angle in the chelated (OC)<sub>4</sub>W(κ<sup>2</sup>-dppm) is 97.3°, not much smaller than that found in **2W** [25]. The P–C–P angle of **5W** is 114.5°, somewhat less than in free vdpp (119.0°).

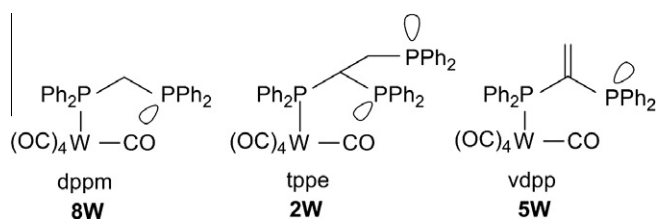
In structures **2W** and **8W** the lone pair of the shorter dangling phosphine arm is directed toward the equatorial W(CO)<sub>4</sub> plane while in **5W**, it is directed away. The M–P...P(lone pair) torsional angles for **2W**, **8W** and **5W** are 61.2°, 26.5° and 166.3°, respectively. The separation between the phosphorus of the uncoordinated phosphine and the closest carbon of the equatorial carbonyls in

**Table 6**  
Selected bond lengths [Å] and angles [°] for **2W**.

W(1)–P(1)	2.5385(19)	O(1)–C(1)	1.142(11)
W(1)–C(1)	2.034(11)	O(2)–C(2)	1.137(11)
W(1)–C(2)	2.041(10)	O(3)–C(3)	1.151(9)
W(1)–C(3)	1.984(8)	O(4)–C(4)	1.125(10)
W(1)–C(4)	2.044(10)	O(5)–C(5)	1.149(10)
W(1)–C(5)	2.031(10)	C(1)–W(1)–P(1)	91.3(2)
C(3)–W(1)–C(5)	90.2(3)	C(2)–W(1)–P(1)	89.9(3)
C(3)–W(1)–C(1)	86.8(3)	C(3)–W(1)–P(1)	178.1(3)
C(3)–W(1)–C(2)	90.1(4)	C(4)–W(1)–P(1)	94.5(2)
C(5)–W(1)–C(1)	86.6(4)	C(5)–W(1)–P(1)	89.8(2)
C(5)–W(1)–C(2)	177.1(4)	O(1)–C(1)–W(1)	175.6(8)
C(1)–W(1)–C(2)	90.5(4)	O(2)–C(2)–W(1)	179.8(11)
C(3)–W(1)–C(4)	87.3(3)	O(3)–C(3)–W(1)	177.1(8)
C(5)–W(1)–C(4)	92.7(4)	O(4)–C(4)–W(1)	172.5(7)
C(1)–W(1)–C(4)	174.1(3)	O(5)–C(5)–W(1)	175.1(8)
C(2)–W(1)–C(4)	90.3(4)		
P(1)–C(6)–P(3)	103.3(4)		

**Table 7**  
Selected bond lengths [Å] and angles [°] for **5W**.

W–C(1)	1.989(7)	O(1)–C(1)	1.145(8)
W–C(2)	2.039(8)	O(2)–C(2)	1.122(8)
W–C(4)	2.042(8)	O(4)–C(4)	1.131(9)
W–C(5)	2.033(7)	O(3)–C(3)	1.133(7)
W–C(3)	2.031(7)	O(5)–C(5)	1.141(8)
W–P(1)	2.530(2)	C(18)–C(19)	1.309(8)
C(1)–W–C(5)	90.4(3)	C(1)–W–C(2)	87.4(3)
C(5)–W–C(2)	89.9(3)	C(1)–W–C(3)	90.8(3)
C(5)–W–C(3)	177.7(2)	C(2)–W–C(3)	88.2(3)
C(1)–W–C(4)	86.6(3)	C(5)–W–C(4)	88.8(3)
C(2)–W–C(4)	173.8(3)	C(3)–W–C(4)	93.2(3)
C(1)–W–P(1)	175.3(2)	C(2)–W–P(1)	97.0(2)
C(3)–W–P(1)	87.6(2)	C(4)–W–P(1)	89.1(2)
C(5)–W–P(1)	91.3(3)	O(1)–C(1)–W	179.5(6)
O(3)–C(3)–W	178.6(5)	O(2)–C(2)–W	176.9(7)
O(4)–C(4)–W	178.4(6)	O(5)–C(5)–W	178.6(5)
P(1)–C(18)–P(2)	114.5(3)		

**Scheme 6.**

**8W** is 3.42 Å. The distance is similar in **2W** where the P(3)–C(4) separation is 3.40 Å, which is less than the sum of the van der Waals radii (1.80 Å + 1.70 Å = 3.50 Å) [26]. The P(3) atom is also relatively close to W (4.07 Å), near the estimated van der Waals radii sum (1.80 Å + 2.26 Å = 4.06 Å). Of the W–C–O angles in **2W**, the W–C(4)–O(4) angle (172.5(7)) deviates most from linearity. In **5W** the separation between P(2) and the closest carbon is 6.21 Å, far greater than would allow for van der Waals interactions.

Significantly, coupling between phosphorus of the short phosphine arm and carbon of the W(CO)<sub>4</sub> plane, <sup>4</sup>J<sub>PC</sub>, is observed in the <sup>13</sup>C{<sup>1</sup>H} NMR spectra for **8W** and **2W** but not for **5W**. The magnitude is larger for **2W** (<sup>4</sup>J<sub>PC</sub> = 3.89 Hz) than for **8W** (<sup>4</sup>J<sub>PC</sub> = 3.00 Hz). When the temperature is lowered from 25 to –30 °C, <sup>4</sup>J<sub>PC</sub> increases to 4.19 Hz in **2W** and 3.20 Hz in **8W**. Long-range P–C coupling is not observed between the axial carbonyl carbon and the uncoordinated phosphines in any of the three complexes, **2W**, **5W** and **8W**.

The <sup>2</sup>J<sub>PP</sub> values for **8W** and **2W** are exceptionally large, consistent with conformation **I**. The value of 106 Hz for **8W** is one of

the largest known for monodentate dppm complexes and matches those for the analogous complexes, (CO)<sub>5</sub>Mo(κ<sup>1</sup>-dppm) (114 Hz) and (OC)<sub>5</sub>Cr(κ<sup>1</sup>-dppm) (94 Hz) [22]. This coupling increases from 106 to 122 Hz at –30 °C. The geminal P–P coupling in **2W** is 207 Hz, a huge value, increasing to 219 Hz at –30 °C and suggesting an enhanced population of conformation **I**. Clearly, a very favorable coupling pathway exists. The <sup>2</sup>J<sub>PP</sub> coupling in **5W** is 68.4 Hz, consistent with coupling in other type **II** conformations. Long range W–P coupling (<sup>3</sup>J<sub>WP</sub>) is observed for **2W** (7.4 Hz) and **8W** (6.3 Hz) but not for **5W** [3].

The single crystal structure of (CO)<sub>5</sub>Mo(κ<sup>1</sup>-dppm) has been reported as well as the <sup>2</sup>J<sub>PP</sub> in a single crystal [21]. The structure is analogous to that of **8W** with a P...C bond distance of 3.44 Å. The solution conformationally averaged <sup>2</sup>J<sub>PP</sub> is 114 Hz. This value increases to 145 Hz in the single crystal where conformation **I** is locked in place. As mentioned above, the <sup>2</sup>J<sub>PP</sub> value for **8W** increases as the temperature is lowered and the predominant conformer becomes more similar to that in the single crystal.

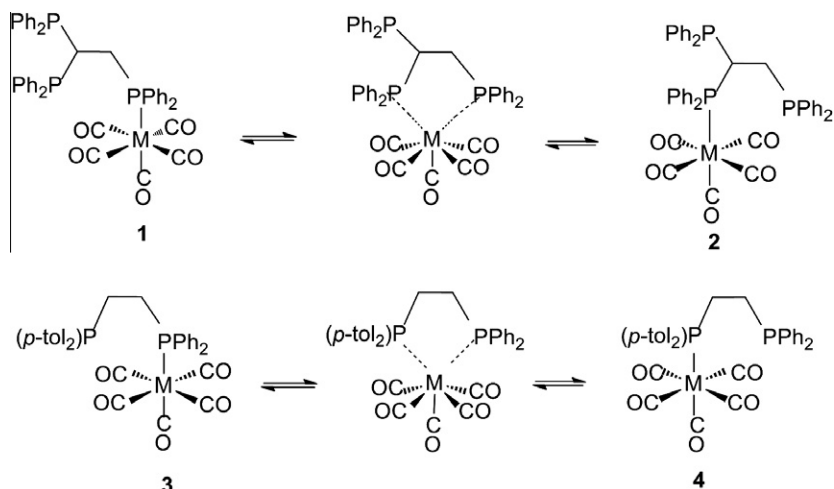
Others have discussed the van der Waals interactions of the R groups in coordinated R<sub>3</sub>P with M(CO)<sub>5</sub>. Medium-range distances between the R group and the equatorial carbonyls lead to attraction while short distances are dominated by repulsive forces [27]. The polar nature of the pendant phosphine arm increases the possibility of a significant van der Waals interaction. The separation between the cis carbonyl carbon and the phosphorus atom of the short dangling phosphine in **2W** and **8W** is much greater than that of a P–C covalent bond (1.8 Å, assuming sp<sup>2</sup> C). Thus, any interaction of a phosphorus lone pair with C–O is weak. While there are a number of examples of nucleophiles (Nu) reacting with metal carbonyls to form stable MC(Nu)O, this is not observed in the ground state of our metal carbonyl complexes [28].

Furthermore, the carbonyl regions of the infrared spectra of **8W** and **2W** show no evidence for deviation from C<sub>4v</sub> symmetry, even at low temperatures, indicating no localized P–CO interaction. In addition, the splitting pattern of the metal carbonyl region of the <sup>13</sup>C{<sup>1</sup>H} spectra is consistent with four equivalent equatorial carbonyl groups. No NMR evidence for a localized carbonyl group was found at temperatures as low as –70 °C.

Structural and spectroscopic observations are consistent with a model for **8W** and **2W** in which the phosphorus lone pair of the shorter dangling phosphine arm has a high probability of interacting with the W(CO)<sub>4</sub> equatorial plane. The close proximity of phosphorus to the carbonyl carbons would allow for an interaction that may well lead to through-space (TS) coupling. The TS coupling could augment the through-bond coupling and increase the <sup>4</sup>J<sub>PC</sub> and <sup>3</sup>J<sub>WP</sub> values. The coupling could arise because of a non-bonded interaction between the phosphorus lone pair and the bonding electrons of the tungsten–carbon bond [29] or because of a very weak donation of the lone pair to an anti-bonding CO orbital [30a]. Non-bonded contacts have been termed “incipient” stages of chemical reactions [30b]. These interactions could also contribute to the extremely large geminal phosphorus–phosphorus coupling. At lower temperatures the interactions become more favorable as the preferred conformations are more highly populated resulting in increased <sup>2</sup>J<sub>PP</sub> and <sup>4</sup>J<sub>PC</sub>. While solid state structures are not available for the tpe complexes of Cr and Mo, NMR results parallel those for tungsten and the same conformational arguments should be applicable.

### 3.4. Mechanism of isomerization

The simplest mechanism to account for the isomerization of the complexes in this study is one which involves a quasi seven-coordinate transition state (Scheme 7) [31]. This simple mechanism is not very satisfying as it does not address the fundamental question of why **1Cr**, **1Mo** and **1W** isomerize 10<sup>4</sup> times faster than **3Cr**, **3Mo**



Scheme 7.

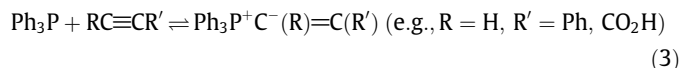
and **3W**. Explanations based on simple electronic or steric effects are inadequate. If steric effects were important one would expect isomerization of **1** to be slower than isomerization of **3**. If electronic effects were important, the more nucleophilic tolyl phosphine arm of **3** would be expected to lead to faster isomerization than observed for **1**.

An alternative mechanism which accounts for the large rate differences observed is one in which a carbonyl group undergoes nucleophilic attack by the dangling phosphine. This in turn leads to a weakening of the metal–phosphorus bond. There are two dangling phosphine arms in **1Cr**, **1Mo** and **1W** but only one in **3Cr**, **3Mo** and **3W**. For the former complexes, one arm is available to interact with the carbonyl group while the second is available for displacing the coordinated phosphine. For both sets of complexes, initiation of the exchange reaction begins with nucleophilic attack on a carbonyl group but for **3Cr**, **3Mo** and **3W**, a 1,2-shift is the only pathway to **4Cr**, **4Mo** and **4W** (Scheme 8).

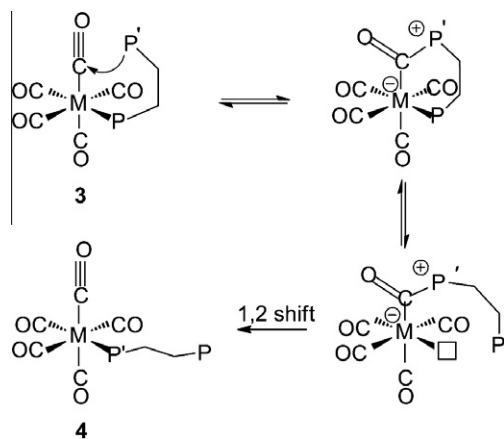
A 1,2-shift would also be possible for **1Cr**, **1Mo** and **1W**, but it is much slower than distal phosphine replacement of the coordinated phosphine with formation of a 5-membered ring. Facile ring opening then gives **2Cr**, **2Mo** and **2W** (Scheme 9).

There is considerable support for the proposed mechanism. Reactions at the CO carbon of metal carbonyls are well-established for hard nucleophiles ( $R^-$ ,  $N_3^-$ ,  $OH^-$ ,  $H^-$ ,  $NH_2OH$ ,  $NEt_2^-$ ,  $PMe_2^-$ ,  $Me_3NO$ ) and plausible for soft nucleophiles [32]. The nucleophilic-

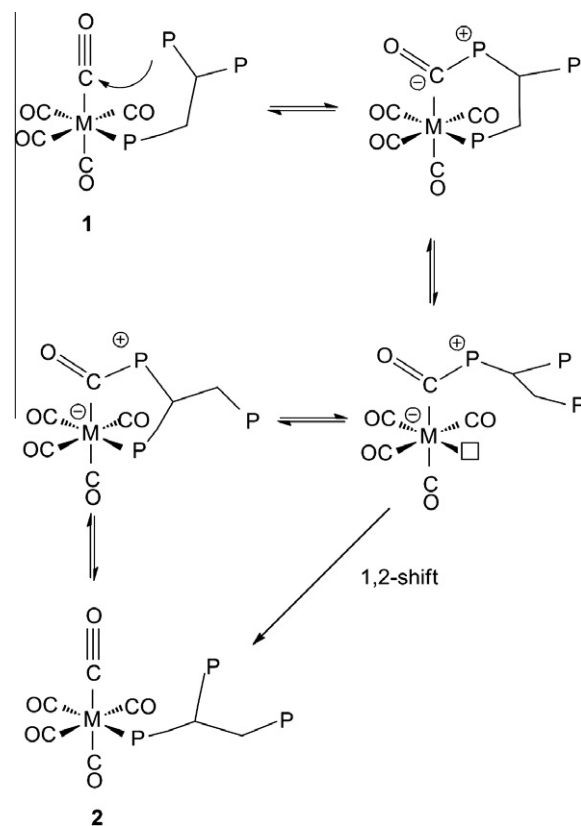
ity exhibited by tertiary phosphines toward  $sp$  hybridized carbon, in general, is significant [33]. For example, reactions with activated alkynes give unstable adducts that typically undergo further reaction.



Adducts also form with isocyanates, activated allenes and carbon disulfide. Alkylidyne complexes in some instances are attacked by  $PMe_3$ . ( $Re\equiv CPh \rightarrow Re=CPhPMe_3$ ;  $W \equiv CPM_3 \rightarrow W=C(PMe_3)_2$  [34]).



Scheme 8.



Scheme 9.

It has been established that the acetate ligand in  $[\text{W}(\text{CO})_5(\text{O}_2\text{CCH}_3)]^-$  is cis-labilizing when  $\text{PR}_3$  replaces a CO ligand to give *cis*- $[\text{W}(\text{CO})_4(\text{PR}_3)(\text{O}_2\text{CCH}_3)]^-$ . It has been suggested that the distal oxygen atom of the acetate ligand interacts with and displaces a cis carbonyl ligand to give *cis*- $[\text{W}(\text{CO})_4(\kappa^2\text{-O}_2\text{CCH}_3)]^-$  as a first step. The solid state structure of  $[\text{W}(\text{CO})_5(\text{O}_2\text{CCH}_3)]^-$  shows that the separation between the distal oxygen atom and the carbon of a cis carbonyl ligand is less than the sum of the Van der Waals radii [35]. Close approaches of pendant thiolate and sulfinate nucleophiles to CO ligands in tungsten pentacarbonyl complexes are viewed as non-bonding but the degree to which they might enhance CO lability is unclear at this point [36].

To account for the oxidation of the terminal phosphine group of  $[\text{Re}_2(\text{CO})_9(\kappa^1\text{-P-P})]$  (P–P = ditertiary phosphine) by  $\text{Me}_3\text{NO}$ , an intramolecular mechanism has been proposed that includes interaction of the uncoordinated phosphine group with a carbonyl ligand. The interaction activates phosphorus for nucleophilic attack by  $\text{Me}_3\text{NO}$ , leading to formation of  $[\text{Re}_2(\text{CO})_9(\kappa^1\text{-P-P=O})]$  [37].

Interaction of a dangling nucleophile with a bound carbonyl group also appears to play a role in facilitating the reaction of CO with the 18-electron  $\text{Cp}^*\text{Ru}[\text{HC}(\text{PPh}_2\text{NPh})_2]$  to give  $\text{Cp}^*\text{Ru}[\text{HC}(\text{PPh}_2\text{NPh})_2\text{CO}]$ . In this instance a Ru–N bond is broken for Ru–CO bond formation and the nitrogen of  $\text{PPh}_2\text{=NRh}$  interacts with the coordinated CO [38].

#### 4. Conclusions

In this work we have presented kinetic, thermodynamic and structural evidence to support a mechanism for exchange of coordinated and uncoordinated arms of di- and tritertiary phosphines in pentacarbonyl complexes of group 6 metals. The initial step involves nucleophilic attack of a pendant phosphine on a carbonyl ligand, leading to dissociation of a coordinated phosphine. The rate-determining step for **3M** is a slow 1,2-shift leading to its linkage isomer, **4M**. For complexes **1M**, a 1,2 shift is also possible but a much faster pathway is available. This entails coordination of the second dangling arm to give a 5-membered ring which opens to give **2M**.

The close approach of a pendant phosphine to the bound carbonyl group in **2W** and **8W** may account in part for the observed 4-bond spin–spin coupling between phosphorus and carbon as well as the 3-bond tungsten–phosphorus coupling.

#### 5. Supplementary material

CCDC 776107 and 776108 contain the supplementary crystallographic data. These data can be obtained free of charge from The Cambridge Crystallographic Data Centre via [http://www.ccdc.cam.ac.uk/data\\_request/cif](http://www.ccdc.cam.ac.uk/data_request/cif).

#### Acknowledgments

We are grateful to Chuck Casey for his keen insight and helpful discussions and to Jeremy Wheeler for assistance in the integration of some P–31 NMR spectra. We thank the Camille and Henry Dreyfus Foundation for a Scholar/Fellow grant (SF-98-004) and the National Science Foundation (CHE-9708342) for support of this work.

#### References

[1] (a) J.D. Atwood, *Inorganic and Organometallic Reaction Mechanisms*, second ed., Wiley-VCH, New York, 1997;  
(b) D.J. Darensbourg, *Adv. Organomet. Chem.* 21 (1982) 113.  
[2] M.J. Wovkulich, J.D. Atwood, *J. Organomet. Chem.* 184 (1980) 77.  
[3] (a) R.L. Keiter, L.W. Cary, *J. Am. Chem. Soc.* 94 (1972) 9232;  
(b) J.A. Connor, J.P. Day, E.M. Jones, G.K. McEwen, *J. Chem. Soc. Dalton Trans.* (1973) 347;

(c) R.L. Keiter, Y.Y. Sun, J.W. Brodack, L.W. Cary, *J. Am. Chem. Soc.* 101 (1979) 2638.  
[4] J.L. Brookham, W. McFarlane, I.J. Colquhoun, *J. Chem. Soc., Dalton Trans.* (1988) 503.  
[5] R.L. Keiter, J.W. Benson, E.A. Keiter, W. Lin, Z. Jia, D.M. Olson, D.E. Brandt, J.L. Wheeler, *Organometallics* 17 (1998) 4291.  
[6] (a) R.L. Keiter, J.W. Benson, Z. Jia, E.A. Keiter, D.E. Brandt, *Organometallics* 19 (2000) 4518;  
(b) K. Maitra, V.J. Catalano, J.H. Nelson, *J. Organomet. Chem.* 529 (1997) 409.  
[7] I.J. Colquhoun, W. McFarlane, *J. Chem. Soc., Dalton Trans.* (1982) 1915.  
[8] (a) S.J. Higgins, B.L. Shaw, *J. Chem. Soc., Dalton Trans.* (1989) 1527;  
(b) G. King, S.J. Higgins, A. Hopton, *ibid* (1992) 3403.  
[9] R.L. Keiter, J.W. Brodack, R.D. Borger, L.W. Cary, *Inorg. Chem.* 21 (1982) 1256.  
[10] W.D. Covey, T.L. Brown, *Inorg. Chem.* 12 (1973) 2820.  
[11] R.J. Angelici, Sister M.D. Malone, *Inorg. Chem.* 6 (1967) 1731.  
[12] H. Schmidbaur, C. Paschalidis, G. Reber, G. Muller, *Chem. Ber.* 121 (1988) 1241.  
[13] J.R. Sowa, R.J. Angelici, *Inorg. Chem.* 30 (1991) 3534.  
[14] J.H. Espenson, *Chemical Kinetics and Reaction Mechanisms*, second ed., McGraw Hill, New York, 1995.  
[15] J.R. Graham, R.J. Angelici, *Inorg. Chem.* 6 (1967) 2082.  
[16] (a) A. Shagal, R.H. Schultz, *Organometallics* 21 (2002) 5657;  
(b) A. Shagal, R.H. Schultz, *ibid* 26 (2007) 4896;  
(c) S. Wieland, R. van Eldik, *Organometallics* 10 (1991) 3110;  
(d) A.W. Ehlers, G. Frenking, *J. Am. Chem. Soc.* 116 (1994) 1514.  
[17] (a) P.B. Dias, M.E. Minas da Piedade, J.A. Martino Simões, *Coord. Chem. Rev.* 135/136 (1994) 737;  
(b) S.L. Mukerjee, R.F. Lang, T. Ju, G. Kiss, C.D. Hoff, S.P. Nolan, *Inorg. Chem.* 31 (1992) 4885.  
[18] G.K. Yang, K.S. Peters, V. Vaida, *Chem. Phys. Lett.* 125 (1986) 566.  
[19] J.L. Brookham, W. McFarlane, M. Thornton-Pett, *J. Chem. Soc., Dalton Trans.* (1992) 2353.  
[20] (a) H. Schmidbaur, G. Reber, A. Schier, F.E. Wagner, G. Müller, *Inorg. Chim. Acta* 147 (1988) 143;  
(b) C. Di Nicola, F.F. Effendy, C. Pettinari, B.W. Skelton, N. Somers, A.H. White, *Inorg. Chim. Acta* 358 (2005) 720;  
(c) R.A. Burrow, F.C. Wouters, L. Borges de Castro, C.eppe, *Acta Crystallogr., Sect. E* 63 (2007) 2559.  
[21] (a) H. Schmidbaur, R. Herr, J. Riede, *Chem. Ber.* 117 (1984) 2322;  
(b) J. Bruckmann, C. Krüger, F. Lutz, *Z. Naturforsch. B* 50 (1995) 351.  
[22] (a) J.W. Benson, R.L. Keiter, E.A. Keiter, A.L. Rheingold, G.P.A. Yap, V.V. Mainz, *Organometallics* 17 (1998) 4275;  
(b) M.E. Rottick, R.J. Angelici, *Inorg. Chem.* 32 (1993) 2421.  
[23] I.J. Colquhoun, W. McFarlane, *J. Chem. Soc.* (1982) 484.  
[24] K. Eichele, G.C. Ossenkamp, R.E. Wasylshen, T.S. Cameron, *Inorg. Chem.* 38 (1999) 639 (The P–C–P angle in  $(\text{OC})_5\text{Mo}(\kappa^1\text{-dppm})$  is also 111°).  
[25] (a) G.W. Wong, J.L. Harkreader, C.A. Mebi, B.J. Frost, *Inorg. Chem.* 45 (2006) 6748;  
(b) G. Hogarth, J. Kilmartin, *J. Organomet. Chem.* 692 (2007) 5655.  
[26] (a) A. Bondi, *J. Phys. Chem.* 68 (1964) 441;  
(b) J.E. Huheey, E.A. Keiter, R.L. Keiter, *Inorganic Chemistry: Principles of Structure and Reactivity*, fourth ed., HarperCollins, New York, 1993. For other van der Waals radii estimates, see:  
(c) R.S. Rowland, R. Taylor, *J. Phys. Chem.* 100 (1996) 7384;  
(d) I.A. Guzei, M. Wendt, *Dalton Trans.* (2006) 3991.  
[27] (a) T.L. Brown, *Inorg. Chem.* 31 (1992) 1286;  
(b) T.K. Woo, T. Ziegler, *Inorg. Chem.* 33 (1994) 1857.  
[28] J.F. Hartwig, *Organotransition Metal Chemistry*, University Science Books, Sausalito, CA, 2010.  
[29] (a) J.-C. Hierro, D. Evrard, D. Lucas, P. Richard, H. Cattey, B. Hanquet, J. Meunier, *J. Organomet. Chem.* 693 (2008) 574;  
(b) J.C. Hierro, A. Fihri, V.V. Ivanov, B. Hanquet, N. Pirio, B. Donnadiou, B. Rebière, R. Amardeil, P. Meunier, *J. Am. Chem. Soc.* 124 (2004) 11077;  
(c) R.H. Contreras, V.A. Barone, J. Facelli, J.E. Peralta, *Ann. Rep. NMR Spectrosc.* 51 (2003) 167;  
(d) B.E. Cowie, D.J.H. Emslie, H.A. Jenkins, J.F. Britten, *Inorg. Chem.* 49 (2010) 4060.  
[30] (a) A.E. Reed, L.A. Curtiss, F. Weinhold, *Chem. Rev.* 88 (1988) 899;  
(b) H.B. Bürgi, J.D. Dunitz, *Acc. Chem. Res.* 16 (1983) 152.  
[31] E.W. Abel, K.G. Orrell, H. Rahoo, V. Sik, *J. Organomet. Chem.* 441 (1992) 441.  
[32] (a) S.W. Kirtley, in: G. Wilkinson, F.G.A. Stone, E.W. Abel (Eds.), *Comprehensive Organometallic Chemistry*, vol. 3, Pergamon Press, New York, 1982;  
(b) E.O. Fischer, F.R. Kreissel, C.G. Kreiter, E.W. Meineke, *Chem. Ber.* 105 (1972) 2558.  
[33] (a) L. Maier, in: G.M. Kosolapoff, L. Maier (Eds.), *Organic Phosphorus Compounds*, Wiley-Interscience, New York, 1972, p. 339;  
(b) H.R. Hudson, in: F.R. Hartley (Ed.), *The Chemistry of Organic Phosphorus Compounds*, John Wiley & Sons, New York, 1990;  
(c) L.D. Quin, *A Guide to Organophosphorus Chemistry*, John Wiley & Sons, New York, 2000.  
[34] (a) W. Uedelhoven, D. Neugebauer, F.R. Kreissel, *J. Organomet. Chem.* 217 (1981) 183;  
(b) A.E. Bruce, A.S. Gamble, T.L. Tonker, J.L. Templeton, *Organometallics* 6 (1987) 1350.

- [35] (a) D.J. Darensbourg, H.P. Wiegrefe, *Inorg. Chem.* 29 (1990) 592;  
(b) D.J. Darensbourg, J.A. Joyce, C.J. Bischoff, J.H. Reibenspies, *Inorg. Chem.* 30 (1991) 1137.
- [36] (a) A.L. Phelps, M.V. Rampersad, S.B. Fitch, M.Y. Darensbourg, D.J. Darensbourg, *Inorg. Chem.* 45 (2006) 119;  
(b) S.P. Jeffery, M.L. Singleton, J.H. Reibenspies, M.Y. Darensbourg, *Inorg. Chem.* 46 (2007) 179.
- [37] W. Fan, R. Zhang, W.K. Leong, C.K. Chu, Y.K. Yan, *J. Organomet. Chem.* 690 (2005) 3765.
- [38] C. Bibal, Y.D. Smurnyy, M. Pink, K.G. Caulton, *J. Am. Chem. Soc.* 127 (2005) 8944.